

REAL-TIME TRACKING CONTROL EMBEDDED WITH BIOLOGICAL NEURONS FOR A CLASS OF MOBILE ROBOTS¹

Shirong Liu^{*}, Simon X. Yang^{**}, Huidi Zhang^{*}

^{*}*Institute of Automation, Ningbo University, Ningbo, Zhejiang 315211, China*

^{**}*School of Engineering, University of Guelph, Ontario N1G 2W1, Canada*

Abstract: A novel stable tracking control scheme with embedded biological neurons is developed for a class of mobile robots. Two individual biological neurons are embedded into the backstepping-based velocity controller to eliminate the *sharp jumps* of linear and angular velocities as the position tracking errors change suddenly. This control system includes a velocity controller and a torque controller. The output of the velocity controller is used as the command input of the torque controller in the control system. The variable structure control based on sliding mode and reaching mode is employed to design the torque controller. The stability of the closed-loop control system can be guaranteed by Lyapunov stability theory. Simulation results demonstrate the effectiveness and efficiency of the proposed control scheme. *Copyright © 2005 IFAC*

Keywords: Biological neurons, mobile robot, stable tracking control.

1. INTRODUCTION

In this paper, we present a stable tracking control system that includes a velocity controller embedded with double biological neurons and a torque controller based on sliding mode and reaching mode. First, a velocity control command produced by a backstepping velocity controller (Kanayama *et al.*, 1990) is used as the control input of a torque controller. Some auxiliary signals generated by biological neurons (Grossberg, 1988) are introduced into the velocity controller to improve the output of the velocity controller. Then a torque controller is used to generate the control torques to control the mobile robot such that the velocities of the robot converge to the desired velocities and the mobile robot follows the desired trajectory. The torque controller is designed by the variable structure control strategy based on sliding mode and reaching mode (Gao and Hung, 1993). The stability of the closed-loop control system is discussed in this paper.

¹This work has been supported by the Natural Science Foundation of Zhejiang Province, China (No. Y104560).

The system with the velocity controller embedded with double neurons can completely eliminate the sharp jumps of linear and angular velocities simultaneously. The proposed system achieves stable and robust tracking control of a mobile robot. Because the passing signals in the system are always bounded smoothly and continuously, the system is able to ensure the mobile robot to navigate safely under any circumstance.

2. PRELIMINARIES

2.1 Modelling of a Nonholonomic Mobile Robot

A nonholonomic mobile robot with n -dimensional generalized coordinate \mathbf{q} subjects to m constraints, and its general kinematics and dynamic equations can be described by the following equations

$$\dot{\mathbf{q}} = \mathbf{S}(\mathbf{q})\mathbf{v}(t) \quad (1)$$

$$\begin{aligned} \mathbf{M}(\mathbf{q})\ddot{\mathbf{q}} + \mathbf{V}_m(\mathbf{q}, \dot{\mathbf{q}})\dot{\mathbf{q}} + \mathbf{F}(\dot{\mathbf{q}}) + \mathbf{G}(\mathbf{q}) + \boldsymbol{\tau}_d \\ = \mathbf{B}(\mathbf{q})\boldsymbol{\tau} - \mathbf{A}^T(\mathbf{q}), \end{aligned} \quad (2)$$

where $\mathbf{M}(\mathbf{q})$ is the symmetric, positive definite mass

matrix, $\mathbf{V}_m(\mathbf{q}, \dot{\mathbf{q}})$ is the centripetal and coriolis matrix, $\mathbf{F}(\dot{\mathbf{q}})$ is the surface friction vector, $\mathbf{G}(\mathbf{q})$ is the gravitational vector, $\boldsymbol{\tau}_d$ is the bounded unknown disturbance including unstructured and unmodelled dynamics, $\mathbf{B}(\mathbf{q})$ is the input transformation matrix, $\boldsymbol{\tau}$ is the input vector, $\mathbf{A}(\mathbf{q})$ is the Jacobian matrix associated with the constraints, and $\boldsymbol{\lambda}$ is the constraint force vector. The matrices and vectors in (1) and (2) have the appropriate dimensions.

A typical nonholonomic mobile robot has two driving wheels mounted on the same axis and a free front wheel (Fierro and Lewis, 1998; Yang and Kim, 1999; Yuan, Yang and Mittal, 2001). Since the surface friction matrix and the disturbance are usually uncertain and unmodelled in practice, we may set $\mathbf{F}(\dot{\mathbf{q}}) = \mathbf{0}$ and $\boldsymbol{\tau}_d = \mathbf{0}$. It is obvious that the gravitational vector $\mathbf{G}(\mathbf{q})$ in the mobile robot is equal to zero, i.e., $\mathbf{G}(\mathbf{q}) = \mathbf{0}$. Set the mass centre C of the mobile robot coincide with the axis centre P of two driving wheels, i.e., $\mathbf{V}_m(\mathbf{q}, \dot{\mathbf{q}}) = \mathbf{0}$. In addition, the dynamic equation (2) can be transformed into a more appropriate form for control purposes, and then the constraint matrix $\mathbf{A}^T(\mathbf{q})\boldsymbol{\lambda}$ in (2) is eliminated. Taking the torque $\boldsymbol{\tau}$ and position \mathbf{q} as the input and output vectors of the mobile robot respectively, the models of a typical nonholonomic mobile robot can be simplified as

$$\dot{\mathbf{v}}(t) = \mathbf{E}\boldsymbol{\tau}(t), \quad (3)$$

$$\dot{\mathbf{q}}(t) = \mathbf{S}(\mathbf{q})\mathbf{v}(t). \quad (4)$$

The input and output vectors and the parameter matrices can be expressed as

$$\mathbf{q}^T = [x_c \ y_c \ \theta], \quad \mathbf{v}^T = [v \ \omega], \quad \boldsymbol{\tau}^T = [\tau_r \ \tau_l]$$

$$\mathbf{S}(\mathbf{q}) = \begin{bmatrix} \cos \theta & 0 \\ \sin \theta & 0 \\ 0 & 1 \end{bmatrix}, \quad \mathbf{E} = \frac{1}{m \cdot r \cdot I} \begin{bmatrix} I & I \\ Rm & -Rm \end{bmatrix},$$

where x_c and y_c are the position of the mass centre of the mobile robot and θ is the orientation with respect to the X-axis in the global coordinates; v and ω are the linear and angular velocities respectively; τ_r and τ_l are the right and left driving torques respectively; m is the mass of the mobile robot, I is the inertia around the mass centre, R is the distance from the axis centre P of two driving wheels to the right or left driving wheel, r is the radius of the driving wheel.

It is required that the velocity and trajectory of the mobile robot can track the given reference velocity and trajectory smoothly and accurately in the tracking control of mobile robots. The reference trajectory $\mathbf{q}_r = [x_r, y_r, \theta_r]^T$ is given by

$\dot{x}_r = v_r \cos \theta_r$, $\dot{y}_r = v_r \sin \theta_r$, $\dot{\theta}_r = \omega_r$, $\mathbf{v}_r = [v_r, \omega_r]^T$, where $v_r > 0$ for all t . According to the transformation between the local coordinates and the

global coordinates, the equivalent trajectory tracking error in the mobile basis frame can be expressed as

$$\mathbf{e}_M = \begin{bmatrix} e_1 \\ e_2 \\ e_3 \end{bmatrix} = \begin{bmatrix} \cos \theta & \sin \theta & 0 \\ -\sin \theta & \cos \theta & 0 \\ 0 & 0 & 1 \end{bmatrix} \begin{bmatrix} x_r - x_c \\ y_r - y_c \\ \theta_r - \theta \end{bmatrix}, \quad (5)$$

where e_1 , e_2 and e_3 are the forward position error, lateral position error and orientation error respectively. Differentiating \mathbf{e}_M with respect to time, the position error dynamics is given by

$$\dot{\mathbf{e}}_M = \begin{bmatrix} \omega e_2 - v + v_r \cos e_3 \\ -\omega e_1 + v_r \sin e_3 \\ \omega_r - \omega \end{bmatrix}. \quad (6)$$

1.2 Biological Neuron Model: Shunting Equation

Hodgkin and Huxley (1952) presented a model for a patch of membrane in a biological neural system using electrical circuit elements. A shunting equation was derived from Hodgkin and Huxley's membrane model (Grossberg, 1988), and is described by

$$\frac{dx_i}{dt} = -A_i x_i + (B_i - x_i) S_i^e(t) - (D_i + x_i) S_i^i(t), \quad (7)$$

where i is the neuron index; x_i is the neural activity (membrane potential) of the i^{th} neuron; A_i , B_i and D_i are the nonnegative constants representing the passive decay rate, the upper and lower bounds of the neural activity respectively; S_i^e and S_i^i are the excitatory and inhibitory inputs to a neuron respectively. The state responses of the model are limited to a finite interval $[-D_i, B_i]$ because of the automatic gain control of the model. It is guaranteed that the neural activity will stay in this region for any amplitude value of the total excitatory or inhibitory input. The stability and convergence of the shunting model has been rigorously proven by Lyapunov stability theory (Grossberg, 1983, 1988).

3. CONTROL SYSTEM DESIGN

The real-time tracking control scheme of a mobile robot is shown in Fig. 1, the velocity and position tracking closed-loop control strategies are adopted. The biological neuron models are introduced into the velocity controller to inhabit or eliminate the sharp speed jumps. In this section, two velocity controllers embedded with a single neuron or double neurons and the torque controller based on sliding mode and reaching mode are presented respectively.

3.1 Velocity Controller Embedded with a Single Neuron

It is well known in robotics that the backstepping technique is a popular design approach for velocity tracking controller. A typical backstepping controller (Kanayama *et al.*, 1990) is given by

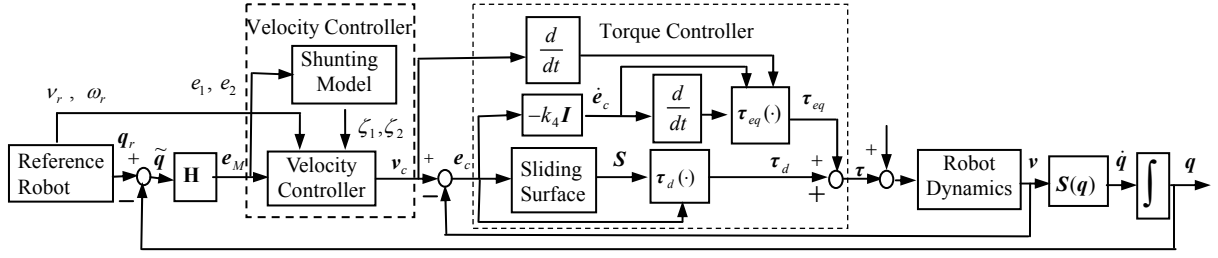


Fig. 1. The scheme of the proposed control system of a mobile robot.

$$\mathbf{v}_c = \begin{bmatrix} v_c \\ \omega_c \end{bmatrix} = \begin{bmatrix} k_1 e_1 + v_r \cos e_3 \\ \omega_r + k_2 v_r e_2 + k_3 v_r \sin e_3 \end{bmatrix}, \quad (8)$$

where v_c and ω_c are the linear and angular velocities respectively, i.e., the outputs of the velocity controller; k_1 , k_2 and k_3 are the positive parameters; v_r and ω_r are the reference linear and angular velocities, respectively.

By the simulation analysis, the velocities of the system exist the *sharp jumping* as the position tracking errors change suddenly, because the errors are directly coupled into (8). It implies that the required acceleration will tend to infinitely large at the sharp jumps, thus this control system is not feasible in practice. Considering the characteristics of the neuron model (7), such as stability, bounded activity and smooth response, we can use the neuron to produce a bounded and smooth auxiliary signal related to the tracking errors to improve the output $v_c(t)$ of the controller (8). A velocity controller embedded with a single neuron was proposed by Yuan et al. (2001), but it was only employed to solve the kinematics tracking problem. A modified velocity controller with a single neuron is proposed, which is an alternate of the controller (8). Set an auxiliary signal v_s generated by a shunting model, and we use it instead of the term $k_1 e_1$ in (8). The velocity controller (8) is modified as

$$\mathbf{v}_c = \begin{bmatrix} v_c \\ \omega_c \end{bmatrix} = \begin{bmatrix} K_s v_s + v_r \cos e_3 \\ \omega_r + k_2 v_r e_2 + k_3 v_r \sin e_3 \end{bmatrix}, \quad (9)$$

where $K_s > 0$, it is an adjustable parameter related to the system stability. Comparing (8) with (9), we can infer that the auxiliary signal v_s should be related to the tracking error e_1 in (5). Thus, let v_s satisfy the following shunting equation

$$\frac{dv_s}{dt} = -A v_s + (B - v_s) f(e_1) - (D + v_s) g(e_1), \quad (10)$$

where $f(e_1) = S^e$ and $g(e_1) = S^i$ are the excitatory and inhibitory inputs respectively, they are defined as

$$f(e_1) = \max\{e_1, 0\}, \quad g(e_1) = \max\{-e_1, 0\}. \quad (11)$$

Because the shunting model is stable, the steady-state value of the equation (10) is

$$v_{ss} = \begin{cases} \frac{B}{A + e_1} e_1 = K^e(e_1) e_1, & \text{if } e_1 \geq 0 \\ \frac{D}{A - e_1} e_1 = K^i(e_1) e_1, & \text{if } e_1 < 0 \end{cases} \quad (12)$$

where the steady-state gains $K^e(\cdot)$ and $K^i(\cdot)$ are positive parameters, which depend on the forward tracking error e_1 except for coefficients A , B and D . The steady-state gains may be considered as an auto-gain-control activity according to the error e_1 . Because of the gains related to e_1 in (12), the shunting model can be viewed as an automatic gain-regulation filter. Due to the symmetry between the excitatory and inhibitory inputs, set $B = D$. Thus, v_{ss} in (12) can be expressed as

$$v_{ss} = K_{ss} e_1, \quad K_{ss} = \frac{B}{A + |e_1|} = \frac{D}{A + |e_1|}, \quad B = D. \quad (13)$$

3.2 Velocity Controller Embedded with Double Neurons

The simulation studies have shown that the modified velocity controller (9) only inhibits the sharp jump of the linear velocity, but the response of the angular velocity has not been improved. Two individual neuron models are used to generate an auxiliary signal vector $\zeta = [\zeta_1 \zeta_2]^T$, which is related to e_1 and e_2 in (5). The auxiliary signals are generated by

$$\dot{\zeta}_i = -A_i \zeta_i + (B_i - \zeta_i) f(e_i) - (D_i + \zeta_i) g(e_i), \quad i = 1, 2. \quad (14)$$

The excitatory and inhibitory inputs are selected as the same as (11). The velocity controller embedded with double neurons is given by

$$\mathbf{v}_c = \begin{bmatrix} v_c \\ \omega_c \end{bmatrix} = \begin{bmatrix} K_1 \zeta_1 + v_r \cos e_3 \\ \omega_r + K_2 v_r \zeta_2 + k_3 v_r \sin e_3 \end{bmatrix} \quad (15)$$

where K_1 and K_2 are the design parameters related to the stability of the control system. In fact, the neuron model (14) is capable of smoothing the position tracking errors. The output of the velocity controller (15) will become smooth even if the position tracking errors change suddenly. Similarly, let $B_i = D_i$ in (14), the steady-state responses are

$$\zeta_{iss} = K_{iss} e_i, \quad K_{iss} = \frac{B_i}{A_i + |e_i|} = \frac{D_i}{A_i + |e_i|}, \quad i = 1, 2 \quad (16)$$

3.3 Torque Controller Based on Sliding Mode and Reaching Mode

It is practically important to design the torque control $\boldsymbol{\tau}(t)$ in addition to the velocity command $\mathbf{v}_c(t)$ designed for the mobile robot. It is a dynamics control issue of nonholonomic systems. As a robust control strategy, the variable structure control (VSC) based on sliding mode has been applied to nonlinear dynamic systems (Utkin, 1993; Gao and Hung, 1993). In general the reaching dynamics of sliding mode is unspecified and uncontrolled. Gao and Hung (1993) suggested that the reaching dynamics of sliding mode should be considered simultaneously in the VSC based on sliding mode. The sliding surface function (Slotine and Li, 1991) and reaching mode (Gao and Hung, 1993) are adopted in the torque controller.

In the velocity closed-loop subsystem, the velocity tracking error is defined as

$$\mathbf{e}_c = [e_4 \quad e_5]^T = \mathbf{v}_c - \mathbf{v}. \quad (17)$$

Differentiating (17) with respect to time and considering the robot's dynamic equation (3), the acceleration error of the system is given by

$$\dot{\mathbf{e}}_c(t) = \dot{\mathbf{v}}_c(t) - \dot{\mathbf{v}}(t) = \dot{\mathbf{v}}_c - \mathbf{E}\boldsymbol{\tau}. \quad (18)$$

A sliding surface function is defined as

$$\mathbf{s}(t) = \begin{bmatrix} s_1(t) \\ s_2(t) \end{bmatrix} = \left(\frac{d}{dt} + \lambda\right)^2 \int_0^t \mathbf{e}_c d\tau, \quad (19)$$

where λ is a positive constant. The time derivative of (19) can be expressed as

$$\dot{\mathbf{s}}(t) = \ddot{\mathbf{e}}_c(t) + 2\lambda\dot{\mathbf{e}}_c(t) + \lambda^2\mathbf{e}_c(t). \quad (20)$$

Substituting (18) into (20), there is

$$\dot{\mathbf{s}}(t) = \ddot{\mathbf{e}}_c(t) + 2\lambda(\dot{\mathbf{v}}_c - \mathbf{E}\boldsymbol{\tau}) + \lambda^2\mathbf{e}_c(t). \quad (21)$$

The reaching law that specifies the dynamics of a sliding surface is defined as

$$\dot{\mathbf{s}} = -\mathbf{Q}\text{sgn}(\mathbf{s}) - \mathbf{D}\mathbf{s}, \quad (22)$$

where $\mathbf{Q} = \text{diag}[q_1, q_2]$, $q_i > 0$, $\mathbf{D} = \text{diag}[d_1, d_2]$,

$d_i > 0$, $\text{sgn}(\mathbf{s}(t)) = [\text{sgn}(s_1) \quad \text{sgn}(s_2)]^T$. Compute the time derivative of $\mathbf{s}(t)$ along the reaching mode trajectory, then from (21) and (22)

$$\ddot{\mathbf{e}}_c(t) + 2\lambda(\dot{\mathbf{v}}_c - \mathbf{E}\boldsymbol{\tau}) + \lambda^2\mathbf{e}_c(t) = -\mathbf{Q}\text{sgn}(\mathbf{s}) - \mathbf{D}\mathbf{s}. \quad (23)$$

The control torque derived from (23) is

$$\boldsymbol{\tau} = \mathbf{E}^{-1} \left(\dot{\mathbf{v}}_c + \frac{\lambda}{2}\mathbf{e}_c + \frac{1}{2\lambda}\ddot{\mathbf{e}}_c \right) + \mathbf{E}^{-1} \frac{1}{2\lambda} (\mathbf{Q}\text{sgn}(\mathbf{s}) + \mathbf{D}\mathbf{s}). \quad (24)$$

The control torque can be rewritten as

$$\boldsymbol{\tau} = \boldsymbol{\tau}_{eq} + \boldsymbol{\tau}_d, \quad (25)$$

$$\boldsymbol{\tau}_{eq} = \mathbf{E}^{-1} \left(\dot{\mathbf{v}}_c + \frac{\lambda}{2}\mathbf{e}_c + \frac{1}{2\lambda}\ddot{\mathbf{e}}_c \right), \quad (26)$$

$$\boldsymbol{\tau}_d = \mathbf{E}^{-1} \frac{1}{2\lambda} (\mathbf{Q}\text{sgn}(\mathbf{s}) + \mathbf{D}\mathbf{s}). \quad (27)$$

In the control law (25), $\boldsymbol{\tau}_{eq}$ is recognized as the equivalent control torque when the tracking error state enters into the sliding plane, and $\boldsymbol{\tau}_d$ is viewed as an additional torque to make sure the tracking error state approaching the sliding plane when the state is far from the switching manifold. Considering the computation difficulty of the term $\ddot{\mathbf{e}}_c$ in (26), the acceleration error is introduced into (26), i.e., define

$$\dot{\mathbf{v}} = \dot{\mathbf{v}}_c + \mathbf{k}(\mathbf{v}_c - \mathbf{v}), \quad \dot{\mathbf{e}}_c = -k_4\mathbf{I}\mathbf{e}_c, \quad k_4 > 0, \quad (28)$$

$$\ddot{\mathbf{e}}_c = -k_4\mathbf{I}\dot{\mathbf{e}}_c. \quad (29)$$

To eliminate chattering completely, it is suggested to use a shifted sigmoid function instead of the sign function in (27), thus $\boldsymbol{\tau}_d$ is computed by

$$\boldsymbol{\tau}_d = \mathbf{E}^{-1} (\mathbf{M}_1\mathbf{h}(\mathbf{s}) + \mathbf{M}_2\mathbf{s}), \quad (30)$$

where $\mathbf{M}_1 = \frac{1}{2\lambda} \text{diag}[q_1 \quad q_2]$, $\mathbf{M}_2 = \frac{1}{2\lambda} \text{diag}[d_1 \quad d_2]$,

$$\mathbf{h}(\mathbf{s}) = [h(s_1) \quad h(s_2)]^T, \quad h(s_i) = \frac{1 - \exp(-s_i)}{1 + \exp(-s_i)}.$$

4. STABILITY ANALYSIS

If the tracking control system of the mobile robot is uniformly asymptotically stable, both the position and velocity errors of the system will converge to zeros, i.e., $\mathbf{e}_M \rightarrow \mathbf{0}$ and $\mathbf{e}_c \rightarrow \mathbf{0}$ as $t \rightarrow \infty$. In Fig. 1, the control scheme includes three parts: the auxiliary signal generator based on biological neuron, the velocity tracking closed-loop subsystem, and the position closed-loop control subsystem that is related to the auxiliary signal generator and velocity tracking subsystem. In the viewpoint of control engineering, the stability of the total system depends on the stability of the individual subsystems. In the velocity tracking subsystem, its closed-loop stability can be ensured by the VSC based on sliding mode and reaching mode. The output boundedness and stability of the auxiliary signals can be guaranteed by Lyapunov stability theory (Grossberg, 1983, 1988). In this section, the stability of the position tracking subsystem is studied by Lyapunov second approach.

The stability of the position closed-loop subsystem with embedded biological neurons is divided to two cases, i.e., with a single neuron or double neurons. For convenience, the auxiliary signal variable ζ_1 is used instead of the variable v_s in (9) and (10).

Assumption 1: The equivalent time constant of the shunting model should be far smaller than that one of the mechanical dynamic system of mobile robot. The transient response process of the shunting equation can end in a short enough time. Thus, the dynamics of the neuron model does not affect the dynamics of the total system.

Assumption 2: The passive decay rate A of the shunting equation can be arbitrarily adjusted so that the equivalent time constant is small enough.

The above assumptions always hold in practice. Consider the position tracking and velocity tracking errors $\mathbf{e}_M = [e_1 \ e_2 \ e_3]^T$ and $\mathbf{e}_c = [e_4 \ e_5]^T$ defined by (5) and (17) respectively, the following Lyapunov function candidate is taken

$$V = (e_1^2 + e_2^2) + 2k_3v_r(1 - \cos e_3) + \frac{1}{2k_4}\mathbf{e}_c^T \mathbf{e}_c, \quad (31)$$

where $V \geq 0$, and $V = 0$ only if $\mathbf{e}_M = \mathbf{0}$ and $\mathbf{e}_c = \mathbf{0}$. The time derivative of V is discussed in two cases, i.e., the velocity controller embedded with a single neuron or double neurons.

Case 1: The System Embedded with a Single Neuron. Using (6), (9) and (28), \dot{V} can be expressed as

$$\dot{V} = 2\dot{e}_1e_1 + 2\dot{e}_2e_2 + 2k_3v_r\dot{e}_3 \sin e_3 - \mathbf{e}_c^T \mathbf{e}_c. \quad (32)$$

$$\begin{aligned} \dot{V} = & 2e_1(-K_s\zeta_1 + e_4) + 2e_2v_r \sin e_3 - e_4^2 - e_5^2 \\ & + 2k_3v_r(e_5 - k_2v_re_2 - k_3v_r \sin e_3) \sin e_3. \end{aligned} \quad (33)$$

Let $k_2 = 1/k_3v_r$, the following result is derived

$$\begin{aligned} \dot{V} = & e_1(e_1 - 2K_s\zeta_1) - (e_1 - e_4)^2 \\ & - (k_3v_r \sin e_3)^2 - (k_3v_r \sin e_3 - e_5)^2. \end{aligned} \quad (34)$$

Taking account of Assumptions 1 and 2, the steady-state response $\zeta_{1,ss}$ of the shunting equation is used

instead of ζ_1 in (34), we obtain

$$\begin{aligned} \dot{V} = & -(2K_sK_{1,ss} - 1)e_1^2 - (e_1 - e_4)^2 \\ & - (k_3v_r \sin e_3)^2 - (k_3v_r \sin e_3 - e_5)^2. \end{aligned} \quad (35)$$

Clearly, if $K_s \geq 1/2K_{1,ss}$, there exists

$$\dot{V} \leq -(2K_sK_{1,ss} - 1)e_1^2 - (e_1 - e_4)^2 - (k_3v_r \sin e_3 - e_5)^2. \quad (36)$$

According to Lyapunov stability theory and LaSalle extension, $\|\mathbf{e}_M\|$ and $\|\mathbf{e}_c\|$ are uniformly bounded.

Case 2: The System Embedded with Double Neurons. Similarly, using (5), (15) and (28), there is

$$\begin{aligned} \dot{V} = & e_1(e_1 - 2K_1\zeta_1) - 2v_r \sin e_3(K_2k_3v_r\zeta_2 - e_2) \\ & - (e_1 - e_4)^2 - (k_3v_r \sin e_3)^2 - (k_3v_r \sin e_3 - e_5)^2 \end{aligned} \quad (37)$$

Under Assumptions 1 and 2, the auxiliary signals ζ_1 and ζ_2 are substituted by the steady-state responses $\zeta_{1,ss}$ and $\zeta_{2,ss}$ in (16), respectively, and there results

$$\begin{aligned} \dot{V} = & -(2K_1K_{1,ss} - 1)e_1^2 - 2v_re_2 \sin e_3(K_2k_3v_rK_{2,ss} - 1) \\ & - (e_1 - e_4)^2 - (k_3v_r \sin e_3)^2 - (k_3v_r \sin e_3 - e_5)^2 \end{aligned} \quad (38)$$

If $K_1 \geq 1/2K_{1,ss}$ and $K_2k_3v_rK_{2,ss} = 1$, there exists

$$\dot{V} \leq -(2K_1K_{1,ss} - 1)e_1^2 - (e_1 - e_4)^2 - (k_3v_r \sin e_3 - e_5)^2. \quad (39)$$

Thus the tracking error norms $\|\mathbf{e}_M\|$ and $\|\mathbf{e}_c\|$ are uniformly bounded according to Lyapunov stability theory and LaSalle extension.

5. SIMULATION RESULTS

An experimental mobile robot (Fierro and Lewis, 1998) is used as a case study to illustrate the performance of the proposed system. Its parameters are $m = 10 \text{ Kg}$, $I = 5 \text{ Kg} \cdot \text{m}^2$, $R = 0.5 \text{ m}$ and $r = 0.05 \text{ m}$. The dynamic tracking problems with the various typical reference paths have been studied by simulations. Here we only discuss the tracking problem of a circular path. The backstepping velocity controller (8), the velocity controller with a single neuron (9) and the velocity controller with double neurons (15) are considered respectively. The design parameters of the control system are given as follows: The backstepping velocity controller (8): $k_1 = 1.5$, $k_2 = 4.5$, $k_3 = 1.5$.

The velocity controller embedded with a single neuron (9): $A_1 = 3.5$, $B_1 = D_1 = 4.5$, $K_s = 1.0$, $k_2 = 4.5$, $k_3 = 1.5$.

The velocity controller embedded with double neurons (15): $A_1 = 3.5$, $B_1 = D_1 = 4.5$; $A_2 = 6$, $B_2 = D_2 = 8$; $K_1 = 1.0$, $K_2 = 1.5$, $k_3 = 1.5$.

The torque controller (25): $k_4 = 25$, $\lambda = 220$, $\mathbf{M}_1 = \text{diag}[0.1 \ 0.1]$, $\mathbf{M}_2 = \text{diag}[0.01 \ 0.01]$.

Consider the reference trajectory be a circular path defined by $x^2 + y^2 = r^2$, $r = 3$. The linear and angular velocities of the reference robot are $v_r = 1.0 \times (1 - \exp(-t/0.5)) \text{ m/s}$ and $\omega_r = v_r / r = 1/3 \text{ rad/s}$, respectively. The reference and actual robots start at $\mathbf{q}_r(0) = [0 \ -3 \ 0]^T$ and $\mathbf{q}(0) = [2 \ -6 \ 0]^T$, respectively. It implies that there are large initial position errors between the reference and actual robots. The control goal is to make the actual robot follow the reference robot motion trajectory perfectly.

The circular tracking trajectories of the control systems are shown in Figs. 2(a)-(c). The linear and angular velocity responses of the systems with the various velocity controllers are given in Figs. 2(d) and (e), respectively. The control torque actions of the individual systems are plotted in Figs. 2(f)-(h). From the simulation results, we can find that the mobile robot with double neurons starts at the initial posture and moves smoothly towards the circular path. The robot catches up the reference path after around 3 seconds, and then follows the reference robot to move, see Fig. 2(a). The responses of linear and angular velocities can track the desired velocities smoothly and continuously without any sharp speed jump, as shown in Figs. 2(d) and (e). The control torque actions of the system are smooth and continuous, and converge to their steady states quickly. Comparing with the other systems, the torque values of the system reach the smallest, see Figs. 2(f)-(h).

The robot with a single neuron also land on the path after around 2.6 seconds and then tracks smoothly the

desired trajectory, and the sharp jump of the linear velocity is completely eliminated, but the response of the angular velocity exhibits very large amplitude in the early moving phase of the robot, see Figs. 2(b), (d) and (e). Comparing with the previous two systems, the robot with the typical backstepping velocity controller only takes about 2 seconds to catch up the circular path, but the robot motion direction has an inversely sudden change at the initial phase, and the linear and angular velocities occur the serious jumps at the beginning, as shown in Figs. (c), (d) and (e). We can find that the torque controller of the system produces in transience the very large sharp control actions in Figs. 2(g) and (h), but it is impossible in practice because of the actuator power limitation. It will result in force impulsion to the mechanical system.

5. CONCLUSIONS

The proposed control system with the velocity controller embedded with double neurons can obtain good performance in position and velocity dynamic tracking without any sharp speed jump for mobile robots. Taking advantages of the robustness of the variable structure control based on sliding mode and reaching mode and the bounded and smooth activity of the biological neurons, the tracking control system achieves stable and robust tracking control of a class of nonholonomic mobile robots. Because all the signals in the system are bounded smoothly and continuously, the control system is able to ensure the mobile robot to navigate safely under any circumstance.

REFERENCES

Fierro, R. and F.L. Lewis (1998). Control of a nonholonomic mobile robot using neural networks. *IEEE Trans. Neural Networks*, **9(4)**, 589-600.

Gao W. and J.C. Hung (1993). Variable structure control of nonlinear systems: A new approach. *IEEE Trans. Industrial Electronics*, **40(1)**, 45-55.

Grossberg, S. (1983). Absolute stability of global pattern formation and parallel memory storage by competitive neural networks. *IEEE Trans. Syst., Man, Cybern.*, **13**, 815-926.

Grossberg, S. (1988). Nonlinear neural networks: principles, mechanism, and architectures. *Neural Networks*, **1**, 17-61.

Hodgkin, A.L. and A.F. Huxley (1952). A quantitative description of membrane current and its application to conduction and excitation in nerve. *J. Phys. Lond.*, **117**, 500-544.

Kanayama, Y., Y. Kimura, F. Miyazaki and T. Noguchi (1990). A stable tracking control method for an autonomous mobile robot. In: *Proc. Int. IEEE Conf. Robotics and Automation*, 384-389.

Slotine, J.J. and W. Li (1991). *Applied Nonlinear Control*. Ch. 7, Prentice Hall, Englewood Cliffs.

Utkin, V.I. (1993). Sliding mode control design principles and applications to electric drives. *IEEE Trans. Industrial Electronics*, **40(1)**, 23-36.

Yang, J.M. and J.H. Kim (1999). Sliding mode control for trajectory tracking of nonholonomic wheeled mobile robots. *IEEE Trans. Robotics and Automation*, **15(3)**, 578-587.

Yuan, G., S.X. Yang and G.S. Mittal (2001). Tracking control of a mobile robot using a neural dynamics based approach. In: *Proc. IEEE Int. Conf. Robotics and Automation*, 163-168.

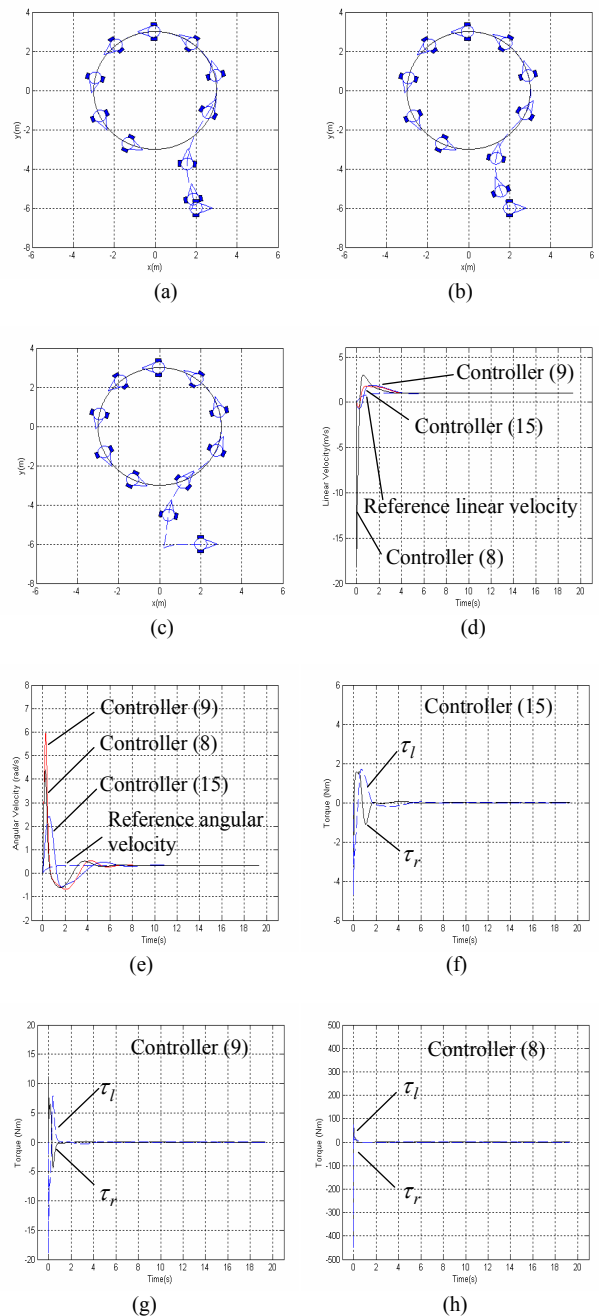


Fig. 2. The trajectory tracking of the mobile robot: (a) tracking trajectory; (b) tracking trajectory; (c) tracking trajectory; (d) linear velocity responses; (e) angular velocity responses; (f) control torques; (g) control torques; (h) control torques.